Electrical Power and Energy Systems 33 (2011) 1410–1419

Contents lists available at ScienceDirect

Electrical Power and Energy Systems

journal homepage: www.elsevier.com/locate/ijepes

Performance and reliability of electrical power grids under cascading failures

Liang Chang [a,*], Zhigang Wu [b]

[a] Mid-America Earthquake Center, University of Illinois at Urbana-Champaign, Urbana, IL 61801, USA
[b] School of Electric Power, South China University of Technology, Guangzhou, Guangdong Province 510640, China

ARTICLE INFO

Article history:
Received 12 February 2010
Received in revised form 17 March 2011
Accepted 3 June 2011
Available online 13 July 2011

Keywords:
Cascading failure
System reliability
Performance
Power grids
Infrastructure
State transition graph

ABSTRACT

The stability and reliability of electrical power grids are indispensable to the continuous operation of modern cities and critical for preparedness, response, recovery and mitigation in emergence management. Because present power grids in China are often running near their critical operation points, they are especially vulnerable and sensitive to external disturbances such as hurricanes, earthquakes and terrorist attacks, which may trigger cascading failures or blackouts. This paper describes a quantitative investigation of the stability and reliability of power grids with a focus on cascading failures under external disturbances. The 118-bus (substation) power network in Hainan, China is employed as a case study to investigate the risk of cascading failure of the regional power grids. System performance and reliability of the power grids are evaluated under two hypothetical scenarios (seismic impact and intentional disturbance) that could trigger cascading failures. By identifying the most vulnerable (critical) edges and nodes, the robustness of the power network is evaluated under the triggered cascading failures. It is found that the system reliabilities could decline as much as 95% during the triggered cascading failure. This paper also explores the use of concepts from modern complex network theories such as state transition graph and characteristic length to understand the complex mechanism of cascading failures. The findings could be useful for power industries and emergency managers to evaluate the vulnerability of power systems, understand the risk of blackout induced by cascading failures, and improve the resilience of power systems to external disturbances.

1. Introduction

Urban infrastructure systems such as power networks are critical backbones of modern societies. The stability and reliability of power networks are indispensible to the continuous operation of modern cities. Because the present power grids are often running near their critical points and these critical infrastructures are attractive target for deliberate attacks [1], power grids are especially sensitive and vulnerable to disturbances such as natural and man-made hazards which could potentially trigger cascading failures. Cascading failure, also known as avalanche of power systems, has drawn intensive research interests in recent years, especially after the large-scale August 14 cascading failure in North America in 2003 [2]. Under extreme events such as natural hazard impact or intentional disruption, failure of power system infrastructure not only disrupts residential and commercial activities, but also impairs post-disaster response and recovery, resulting in substantial socio-economic consequences [2–9].

Evaluation of the performance and reliability of infrastructure systems is complex in nature due to the large number of network components, complex network topology [10], and component/system interdependency [11]. Currently, the most successful study of power network cascading failures is based on the OPA and CASCADE models [12–14]. Although some results can be drawn based on these models, it is still difficult to explain whether and how an external disturbance can cause a cascading failure [15].

Complex system theories have been recently employed to understand cascading failures [5,16–18]. Watts showed that the topology of modern power grid is always a small-world graph and the propagation of failures within the network can be studied using complex system theories [16]. Focusing only on the topologies of power systems, these approaches, however, ignored the weights of nodes (generators and substations) and links (transformers and transmission lines), which could be of more importance in practice [5,15]. For instance, stakeholders and emergency managers are often concerned about the availability of electricity services, or the connectivity between power generator and service areas. Network reliability, or the probability of connectivity between node-pairs can be evaluated based on the network configuration with system reliability theories.

For lifeline networks, system reliability can be measured in three perspectives [19]: (1) reliability of structural components; (2) connectivity reliability between node-pairs; and (3) system performance reliability, i.e., keeping infrastructure equipments from overloading or maintaining minimum water head (pressure)

* Corresponding author. Present address: Risk Management Solutions, Inc., 7575 Gateway Blvd., Newark, CA 94560, USA. Tel.: +1 510 505 2578; fax: +1 510 505 2501.

E-mail address: liang.chang@rms.com (L. Chang).

0142-0615/$ - see front matter © 2011 Elsevier Ltd. All rights reserved.
doi:10.1016/j.ijepes.2011.06.021

for serviceability requirements. In this paper, the scope of reliability analysis presented is limited to system-level connectivity reliability and the reliability of overloaded equipment is not discussed.

The underlying idea of analytic network reliability method is to convert complex network to combination of simple networks such as parallel or series systems, and then system reliability could be computed by finding the union and intersection of these simple networks, e.g. a generic substation can be modeled with a series system of macro-components [20]. Kroft [21] first described a shortest path algorithm to compute system reliability. Panoussis [22] and Taleb-Agha [23,24] proposed that general network reliability can be computed by converting complex lifeline networks to SSP (series systems in parallel) networks. However, finding the shortest paths is not always an easy task, especially for large-scale networks. Aggarwal and Misra [25] proposed disjoint shortest path algorithm. Later, this algorithm was improved to give exact reliability for large-scale complex networks [26–29]. The full probability analytic algorithm [30] and ordered binary decision diagram (OBDD) algorithm [31] are also able to find exact network reliability but neither is able to handle large-scale networks.

On the other hand, since complete information is not always available, especially for complex systems, researchers chose to describe the system reliability approximately with reliability bounds [32]. But the theoretical bounds are often too wide for practical uses until much narrower reliability bounds of the reliability of power substation systems were obtained by linear programming [33,34]. Recently, a matrix-based system reliability (MSR) method was developed to estimate the system reliability of infrastructure systems [35]. MSR is easy to implement and flexible to handle dependence and incomplete information [36].

This paper studies the cascading failure of the power system with the specific emphasis on its stability and network reliability. First, the stability performance is evaluated with the state transition graph. Next, the system reliability of the power system under cascading failures is analyzed. A provincial power network in China is used as a numerical example to demonstrate the analysis. The results and observations from the case study are summarized, and the identified future research topics are also presented.

2. Performance and the state transition graph of power grids

The capability of power grids to deliver electric power depends on boundary conditions (e.g., power and voltage from supply nodes and to demand nodes), admittance of transmission lines, and working states (operating or failure) of substation components.

Boundary conditions are specified at the nodes in terms of active and reactive components at the load nodes, real power and voltage amplitude at the generation nodes, and voltage amplitude and phase angle at the swing node. In general, the steady state of a power system is described by power flow, which is the solution of a typical nonlinear equation sets:

$$\dot{\mathbf{V}}\overset{*}{\mathbf{Y}}\overset{*}{\mathbf{V}} = \dot{\mathbf{S}} = \mathbf{P} + j\mathbf{Q} \tag{1}$$

where $\dot{\mathbf{V}}$ is the voltage phasor vector as a complex value; $\mathbf{Y}$ is the admittance matrix corresponding to the power network; $\dot{\mathbf{S}}$ is the vector of complex power injected into each nodes; $\mathbf{P}$ is active power (real part); $\mathbf{Q}$ is reactive power (imaginary part); "$*$" is the conjugate operator.

Electrical power transferred through a given edge (i.e., transmission line or transformer) can be calculated once the power flow equation is solved. The power flow model is theoretically appropriate since the power system runs normally for most of time, and most blackouts always happen with a long-period dynamics, which can also be described by power flow [37].

Power grids can be treated as a weighted digraph from a macroscopic viewpoint: generators and load motors as the nodes to inject electric power and loads into power grids, and transmission lines and transformers as the edges to transfer electrical power. To quantify the security of power system, the capacity factor of each edge other than mere electrical power is taken as the edge weight. For example, the weight of a transformer is the ratio of apparent power transferred over its rated capacity, while the weight of a transmission line is usually the ratio of actual transmitted current over its rated current.

Though most electrical equipments are designed with overloading protection capacities, it is assumed that the overloaded equipments shall quit the network and the working state be "failure", and vice versa. Electrical power grid can be treated as a discrete dynamical network when all buses, transmission lines, and transformers have binary working states, that is, operating state denoted by "1" and failure state by "0". By describing the states of nodes and edges with binary vectors, state transition graphs [15,38] can capture dynamic behaviors of both nodes (i.e., power plants and substations) and edges (e.g., transmission lines) and can be used to illustrate the cascading failure of power networks. In nature, the state transition graph is an enumeration of all possible initial states of the system. Since it is often computationally expensive to employ state transition graphs directly especially for large networks, the characteristic lengths of state transition graphs provide us an alternative measure to understand cascading failures. The global behavior of state transition graph can be illustrated with the characteristic length of the graph:

$$l = \frac{1}{n(n+1)/2}\sum_{i \geqslant j} d_{ij} \tag{2}$$

where l is the characteristic length of the graph, measured by the *average distance* between arbitrary two nodes in the graph; d_{ij} is the length of the shortest path between node i and node j. The characteristic length of a graph can be used to evaluate the possibility of state transitions of power grids [15].

3. System reliability under cascading failures

This paper employs the MSR method to assess the system reliability of power networks. The MSR method subdivides the sample space of component events with s_i distinct states, $i = 1, \ldots, n$, into $m = \Pi_{i=1}^{n} s_i$ mutually exclusive and collectively exhaustive (MECE) events. The probability of any general system event is then described by the inner product of two vectors:

$$P(E_{sys}) = \mathbf{c}^{\mathrm{T}}\mathbf{p} \tag{3}$$

where $\mathbf{c}$ is the "event vector" whose element is 1 if its corresponding MECE event is included in the target system E_{sys} event, and 0 otherwise; and $\mathbf{p}$ is the "probability vector" that contains the probabilities of all the MECE events. Efficient matrix-based procedures [39] were proposed to efficiently obtain these vectors by use of matrix computing languages such as Matlab.

The MSR method has the following merits over existing system reliability methods. First, the probability of a system event is always calculated by a simple matrix multiplication as in Eq. (3) regardless of the complexity of the system event definition. Second, the MSR method separates the tasks of identification of system event ($\mathbf{c}$) and computation of probability calculations ($\mathbf{p}$), which allows for an easy integration with other computation modules, e.g. geographic information system (GIS) or network analysis algorithms. Moreover, the matrix-based procedures proposed along with the method help obtain $\mathbf{c}$ and $\mathbf{p}$ vectors efficiently. Third, even if one has incomplete information on the component failure probabilities and/or their statistical dependence, the matrix-based framework is still able to obtain the narrowest possible bounds on any general system event [32] based on the available information. Fourth, once $P(E_{sys})$ is obtained, one can calculate the probabilities of other system events of interest, conditional probabilities and component importance measures [40] without additional probability calculations.

It is worth noting that the size of the vectors increases exponentially with the number of component events. This may be a critical issue in case a network with a large number of components is considered. However, this can be overcome by a multi-scale approach [41] or subdividing the system event into multiple disjoint link sets or cut sets constituted by smaller number of components. When disjoint cut sets or link sets, S_i, $i = 1, \ldots, N_{set}$ are identified, the system failure probability or reliability is computed by summing up the results of the MSR analyses of individual sets, i.e.,

$$P(E_{sys}) = \sum_{i=1}^{N_{set}} P(S_i) = \sum_{i=1}^{N_{set}} \mathbf{c}_i^{\mathrm{T}} \mathbf{p}_i \tag{4}$$

where $\mathbf{c}_i$ and $\mathbf{p}_i$ are the event and probability vectors of the ith disjoint cut set or link set [35]. These disjoint sets can be efficiently identified by making use of an advanced network algorithm such as the recursive decomposition algorithm (RDA) [29].

RDA recursively decomposes the network into sub-graphs until there exists no paths between the source and terminal nodes in all sub-graphs. When paths between source and terminal are found in sub-graphs, they are disjoint link sets in nature and thus contribute to the network reliability; for those sub-graphs containing no paths, they are disjoint cut sets that contribute to the system failure probability. RDA is applicable to all types of networks regardless of their size or topology.

After the Boolean descriptions of the disjoint cut sets and link sets are identified, the corresponding event vectors $\mathbf{c}_i$'s are obtained by use of the following matrix-based procedures [39]:

$$\begin{aligned} &\mathbf{c}^{\bar{E}} = \mathbf{1} - \mathbf{c}^{E} \\ &\mathbf{c}^{E_1 \cdots E_n} = \mathbf{c}^{E_1} .^{*} \mathbf{c}^{E_2} .^{*} \cdots .^{*} \mathbf{c}^{E_n} \\ &\mathbf{c}^{E_1 \cup \cdots \cup E_n} = \mathbf{1} - (\mathbf{1} - \mathbf{c}^{E_1}) .^{*} (\mathbf{1} - \mathbf{c}^{E_2}) .^{*} \cdots .^{*} (\mathbf{1} - \mathbf{c}^{E_n}) \end{aligned} \tag{5}$$

where $\mathbf{1}$ denotes a vector of 1's; and ".*" is the Matlab® operator for element-by-element multiplication.

When component events are statistically independent of each other, the probability vectors $\mathbf{p}_i$'s are constructed based on the failure probabilities of the lifeline network elements by the following recursive matrix-based procedure:

$$\begin{aligned} &\mathbf{p}_i^{[1]} = [P_1 \quad 1 - P_1]^{\mathrm{T}} \\ &\mathbf{p}_i^{[j]} = \begin{bmatrix} \mathbf{p}_i^{[j-1]} \cdot P_j \\ \mathbf{p}_i^{[j-1]} \cdot (1 - P_j) \end{bmatrix} \quad \text{for } j = 2, 3, \ldots, n_i \end{aligned} \tag{6}$$

where n_i is the number of components in the ith cut set or link set, P_j is the failure probability or reliability of the jth component in the set; and $\mathbf{p}_i = \mathbf{p}_i^{[n_i]}$. The probability vectors can be obtained even in case the components have statistical dependence [39].

4. Case study: the hainan regional power grids

Electrical equipments of power grids are vulnerable and could be damaged under extreme events, which may trigger cascading failure even a regional blackout. For example, the magnitude 8.8 Chile earthquake on February 27, 2010 damaged the Chilean Central Interconnected System (SIC) and an immediate blackout took place that affected four and a half million population [42]. Two weeks later, a blackout resulted from the failure of a 500 kV transformer and affected about 90% of the entire population of Chile on March 14, 2010. The Chilean government believed this blackout was a consequence of the February 27, 2010 earthquake.

In this case study, Hainan, a Chinese province with a population of more than 8.26 million [43] in South China is taken as the target region. The Hainan power grids were severely damaged by Typhoon Damrey on September 26, 2005, resulting in an island-wide blackout for about 48 h and significant economic loss of more than 11.6 billion RMB [6]. The state-owned Hainan Power Grid Company (HPGC), part of the China Southern Power Grid (CSPG), provides electricity services to more than 1.36 million customers in this area [44].[1] The electrical facilities operated by HPGC cover more than 33,920 square km service territory through more than 1339 km of 220 kV transmission lines and more than 5015 km of distribution lines. The HPGC power grid consists of 118 buses (substations) and more than 180 branches (transformers and transmission lines). The total installed capacity is 3850 MW, with the peak load of 1891 MW. For the purposes of demonstrating the methodology without undue complexity, a simplified power network model in Fig. 1a is used, which consists of 48 nodes (thermal power plants and substations) and 59 links (transmission lines). Note that only the 19 thermal power units are considered to be supply facilities or source nodes for the given power network. The power transmission lines are taken as distributing elements while the substations as demand nodes. Since power networks less than 110 kV are usually taken as distribution networks, all the loads are assumed to be connected directly to the 110 kV buses. Although the network used in this research only contains 107 elements, a multi-scale approach [41] can be used to assess the system reliability by aggregating or disaggregating service areas into equivalent service nodes.

A directed graph model (shown in Fig. 1a) is used to represent the HPGC network. The arrows indicate the directivity of electric current flow, i.e., from sources to customers, and from high voltage substations to low voltage ones. As shown in Fig. 1b, a subjunctive source node feeding all power plants is added to the directed graph model to facilitate finding the node-pair connectivity in the multi-source network [29].

Electrical equipments in power grids usually have different operating reliabilities. Even for the same type of equipments, their reliability may not be identical. For demonstration purposes, the reliability of electrical equipments is assumed identical (0.95) in this numerical example. When accurate information of equipment reliabilities is available later, it can be used to get refined results.

The event vector ($\mathbf{c}$) and probability vector ($\mathbf{p}$) are obtained for each link set or cut set by use of matrix-based procedures as described in Eqs. (5) and (6). The probability of outage at each distribution node, i.e. its disconnection from all the sources is computed by Eq. (4).

System reliability of the HPGC network is evaluated under two hypothetical scenarios, in which the power grids are under an intentional disruption or seismic impact. System performance of the target power grids is evaluated by analyzing the characteristic length of state transition graphs.

4.1. Scenario 1: intentional disruption

In this intentional disruption scenario, it is assumed the consequences of disruption on a particular node are substantial so that the node is completely damaged and its adjacent edges quit from the system immediately after the attack, which is equivalent to deleting the node and its adjacent edges from the network by changing the network's topology.

[1] The HPGC power system analyzed in this paper is connected to the Chinese mainland power system via a submarine cable in June 2009. The reliability of this system should be significantly improved but requires to be further studied when new data is available.

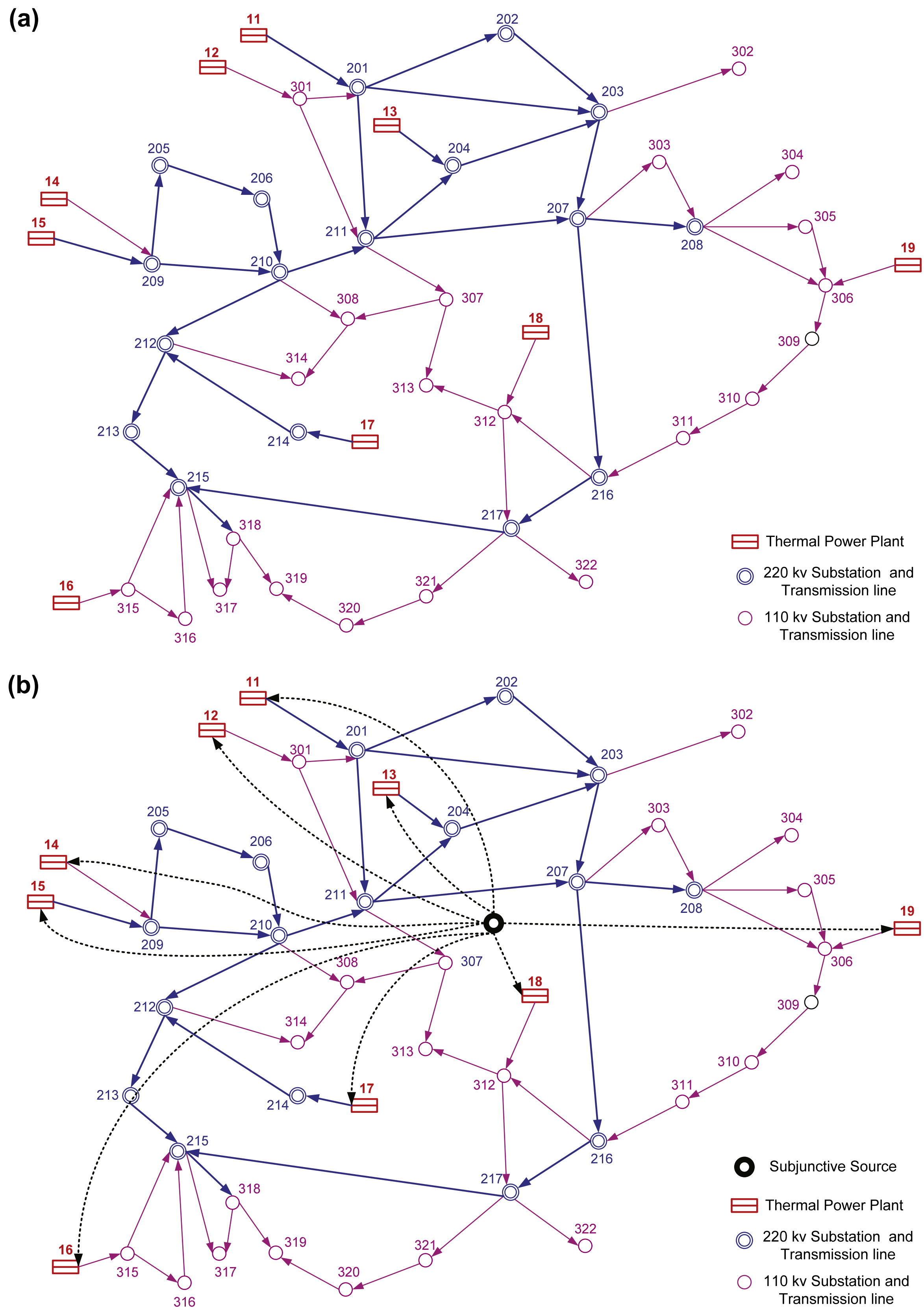

Fig. 1. Graph model of HPGC power grid. (a) Directed graph model and (b) graph model with the subjunctive source node.

As shown in Fig. 2a, a 220 kV substation (substation 208) is assumed to be the target of intentional disruption. The attack resulted in the immediate failure of substation 208, followed by a series of cascading failures in the eastern part of the study area.

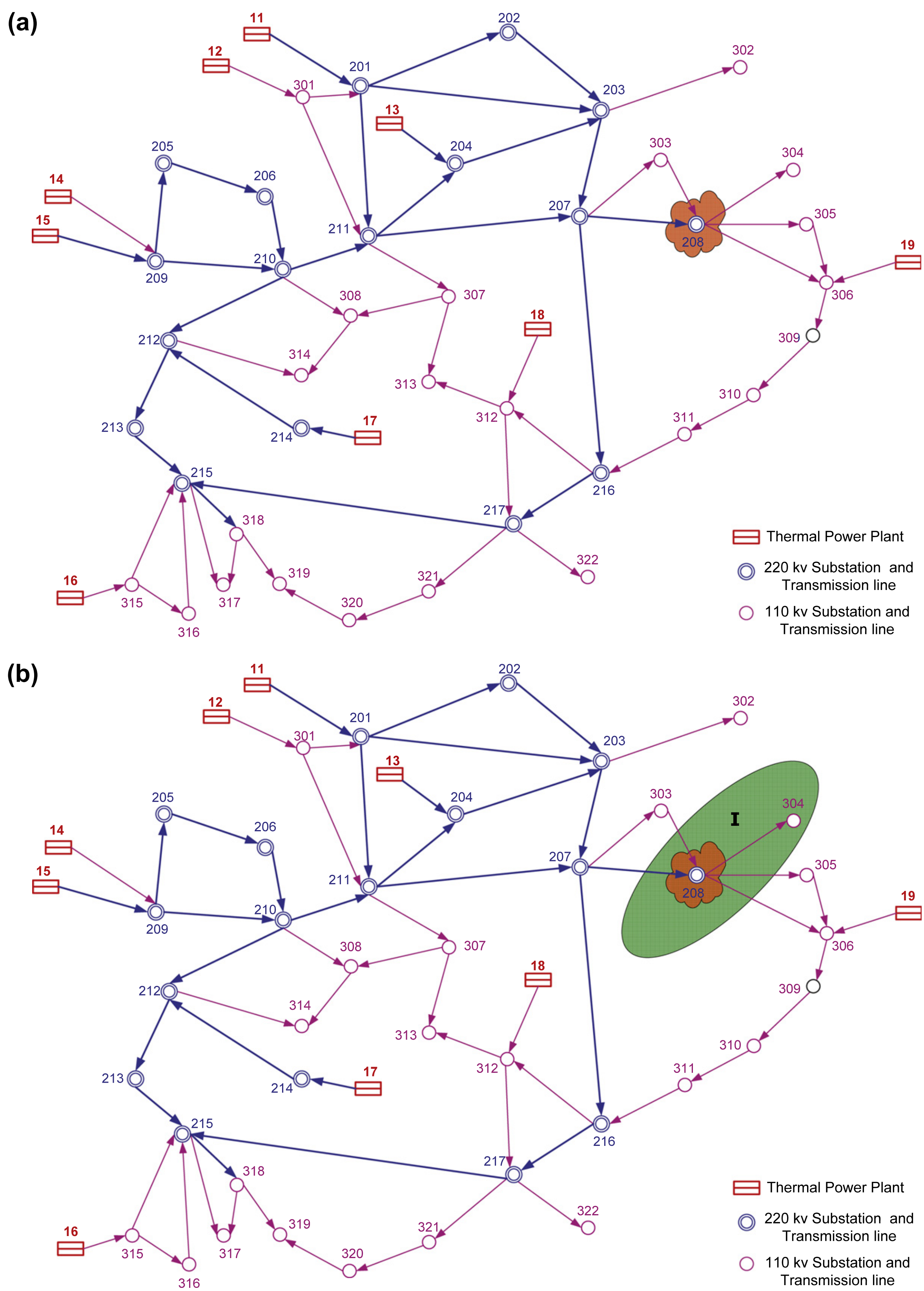

Fig. 2. Cascading failure of the HPGC power network under intentional disruption. (a) Intentional disruption to substation 208 (number of failed buses = 1, number of failed AC lines = 0, load under outage = 0 MW). (b) Phase I: substation 304 failed and quitted the network (number of failed buses = 2, number of failed AC lines = 5, load under outage = 138.3 MW). (c) Phase II: three more substations (305, 306 and 309) and power plant 19 failed and quitted the network (number of failed buses = 5, number of failed AC lines = 8, load under outage = 564.6 MW). (d) Phase III: two more substations (310 and 311) failed and quitted the network (number of failed buses = 7, number of failed AC lines = 11, load under outage = 645.3 MW). System reached to a stable state after Phase III.

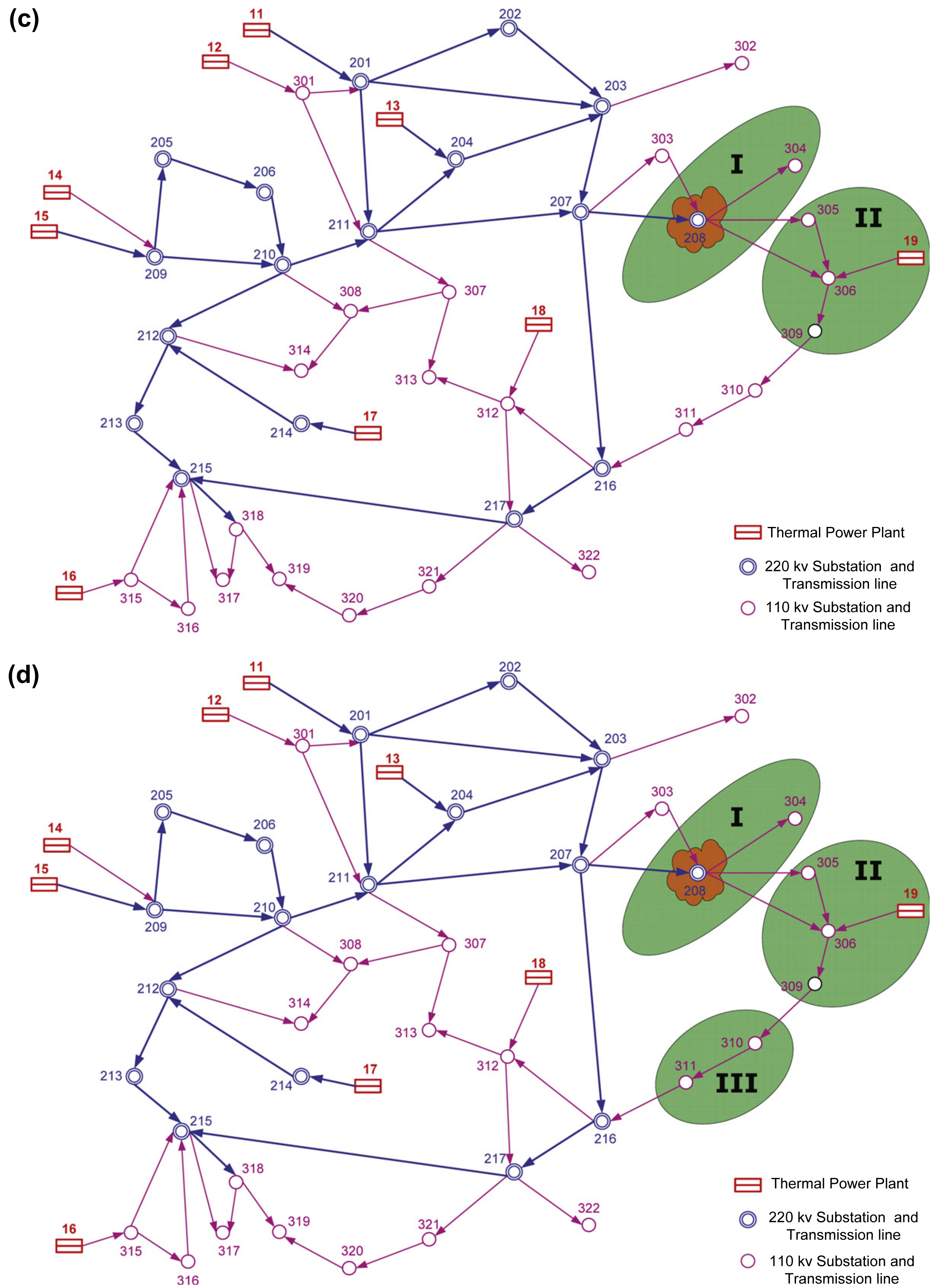

Fig. 2 (*continued*)

The three-phase cascading failure propagated on the power network and changed the network topology. Fig. 2 illustrates details of each phase during the cascading failure.

In the first phase, substation 304 quitted working from the network due to the failure of substation 208. Subsequently, power plant 19 and three 110 kV substations (i.e., substations 305, 306, and 309) failed and service regions covered by these facilities experienced a power outage. In the last phase of the cascading failure, substations 310 and 311 stopped operating since the only power source (substation 306) feeding these two substations failed in

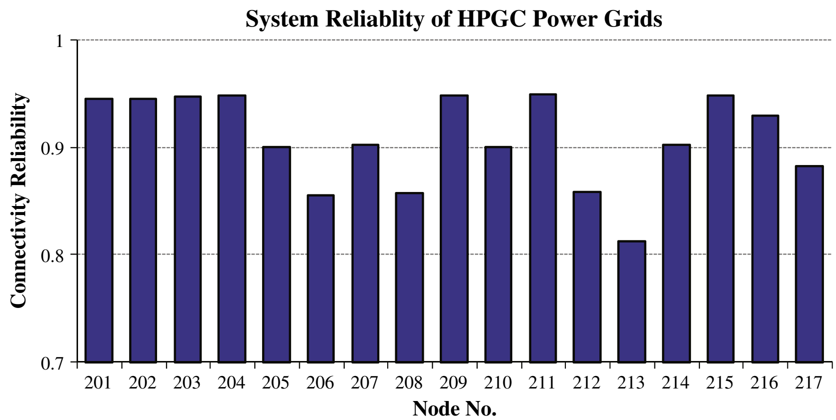

Fig. 3. System connectivity reliability of network nodes.

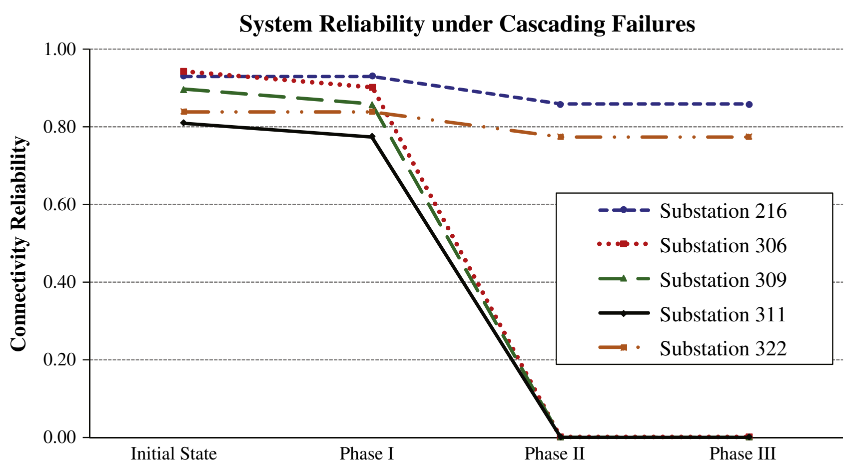

Fig. 4. System reliability under cascading failures.

the second-phase cascading failure. Redistribution of power flow with the new network topology is calculated in each phase of the cascading failures. Power flow over the girds reached a stable state when the system equilibrium equations reached convergent solutions after the three-phase cascading failure.

Fig. 3 shows the post-event network reliability using RDA and the MSR method while Fig. 4 illustrates the connectivity reliability (P_{sys}) of several selected nodes to the sources in each phase of the cascading failures. Note that the disconnection probability ($1 - P_{sys}$) of these nodes increases as the outage propagates over the power network, which parallels to one's intuitive reasoning. The downstream nodes 306, 309, and 311 have the highest outage potential in the triggered cascading failure—the system reliabilities at these nodes declined as much as 95% during the cascading failure, while nodes 216 and 322 are less prone to the cascading failure with relatively small changes of system reliability.

4.2. Scenario 2: seismic impact

For illustrative purposes, a magnitude 7.0 event is assumed to occur with the epicenter at the location of 220 kV substation 208 in the hypothetical earthquake scenario. Since the development of attenuation relationship is out of the scope of this paper, a simple circular ground motion attenuation relationship [5] was used to determine the distribution of ground motion intensity (e.g., PGA) at each site on the HPGC network.

Structural fragility curves are essential for evaluating the seismic reliability of electrical equipments such as substations under earthquake impact. Structural fragility, also known as damage function, is defined as the conditional probability that the condition of a structure exceeds the prescribed structural limit state LS_i (e.g., significant damage or collapse) for a given ground motion intensity (e.g., taking peak ground acceleration, PGA as the intensity measure). As an example, the analytical fragility curve can be given as:

$$P(LS_i|PGA = a) = \Phi\left(\frac{\ln a - \lambda_i}{\beta_i}\right) \tag{7}$$

where $\Phi(\cdot)$ is the cumulative density function of the standard normal distribution, a is the ground motion intensity, and λ_i and β_i are the median and dispersion of the lognormal distribution, respectively, for the ith limit state of a particular structural type.

Seismic reliability of electrical equipments are often developed using structural experiments in conjunction with computer simulations. The development of such structural fragility curves falls outside the scope of this paper and detailed procedure can be found in [20,45–48]. Since the focus of this paper is to examine the overall system performance and reliability instead of concentrating on the vulnerability of network components, the generic structural fragility curves from [20] are employed to estimate the seismic reliability of substations under earthquake impact.

Using the attenuation relationship and fragility curves, it is found that six substations (i.e., substations 208, 303, 304, 305,

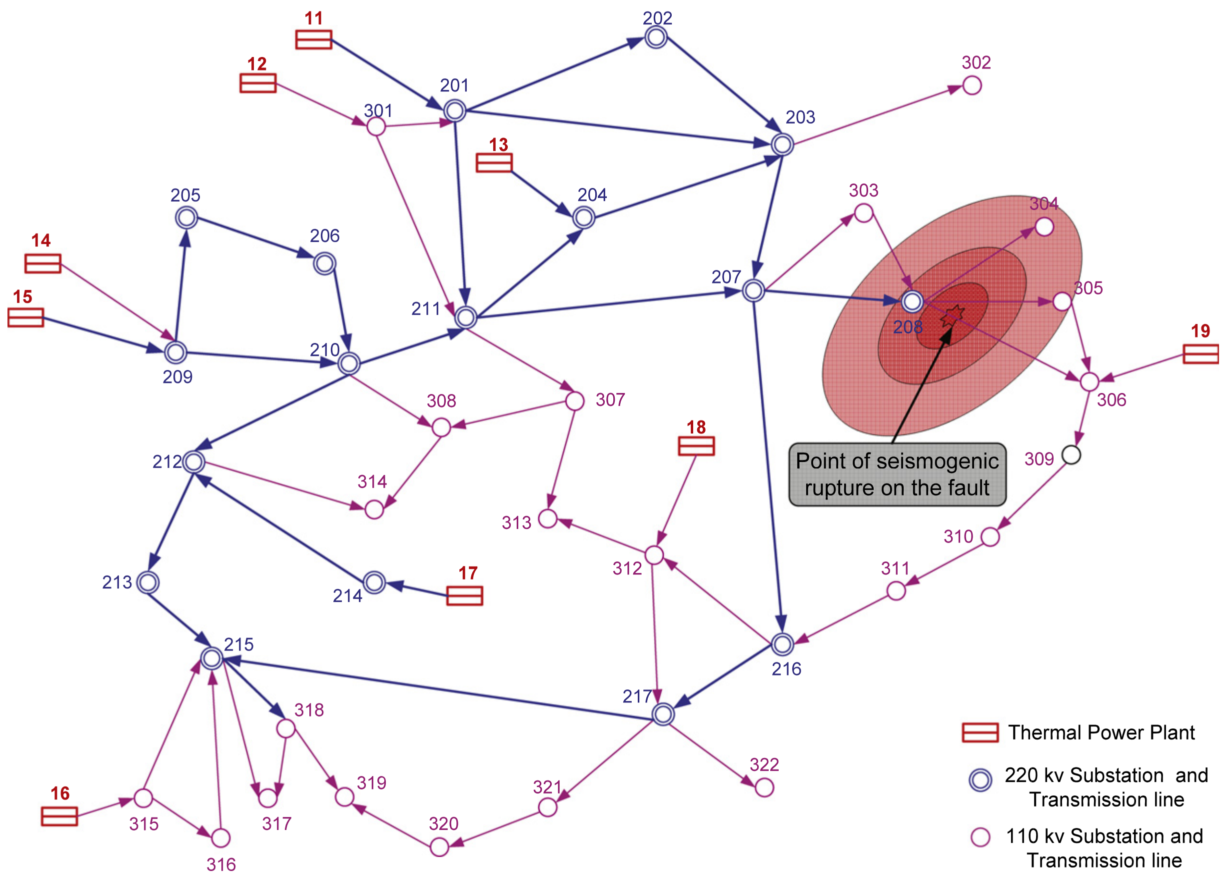

Fig. 5. HPGC power network under earthquake impact (Number of failed buses = 3, Number of failed AC lines = 5, Load under outage = 322.7 MW).

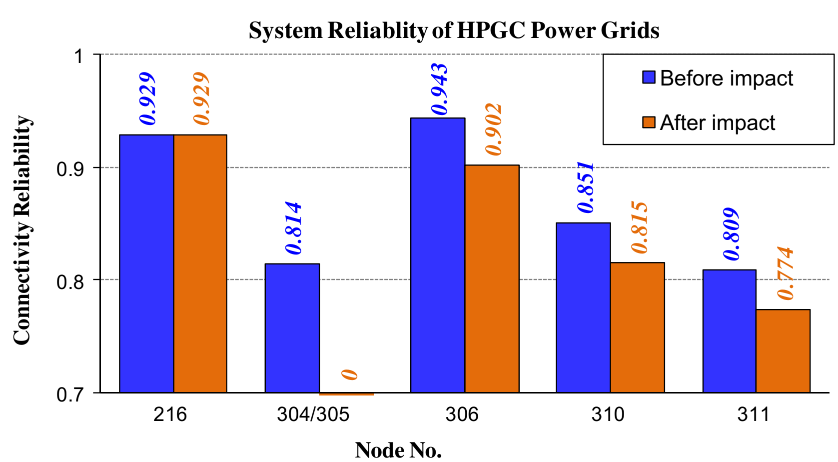

Fig. 6. System reliability under cascading failures.

306 and 309 in Fig. 5) are located in high seismicity regions (where intensity larger than 7). Under the hypothetical seismic impact, three substations (208, 304, and 305) failed due to excessive structural damage and quitted from the network. Convergent solution was reached after five iterations by changing the topology of damaged network and recalculating the power flow—the system operated stably with the partially damaged power grids. Unlike Scenario 1, the power grids are robust under the earthquake impact: the effect of seismic damage did not propagate over the power network and no cascading failure occurred in Scenario 2. Fig. 6 compares the system reliability of selected substations before and after the earthquake impact. The system reliability of seismically damaged nodes decreased significantly, indicating high vulnerability of power grids in the strong intensity regions.

4.3. Performance of the power systems

To simulate the cascading failure of power grids, a 6-step cascading failure simulation algorithm is utilized. This simulation algorithm captures the state changes from disturbances and illustrates the cascading failure as the state transition graph [15]. Since

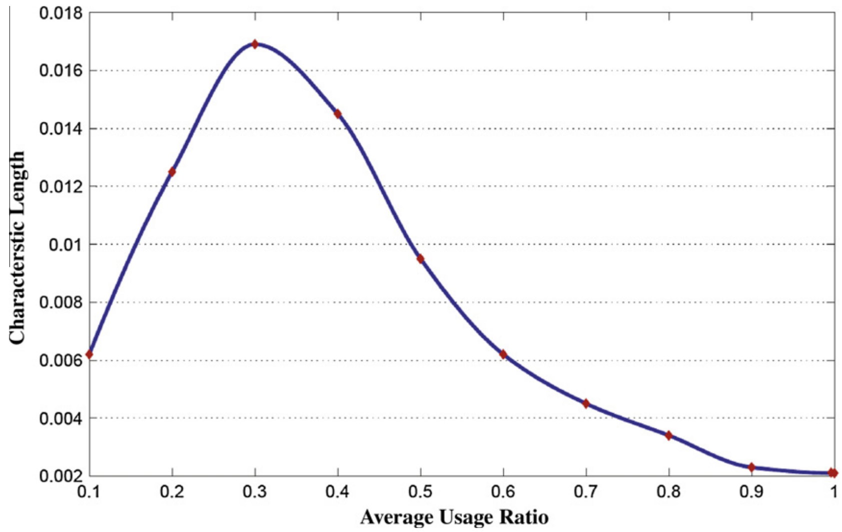

Fig. 7. Characteristic length of state transition graph of the HPGC power network with various average usage ratios.

there are more than $2^{118+180} \approx 5 \times 10^{89}$ states in the state space, it is infeasible to show all the states in a single state transition graph. However, the global behavior of the state transition graph can be illustrated with the characteristic length of the graph described in Eq. (2).

Fig. 7 illustrates the characteristic length of state transition graph at various average usage ratios of the HPGC power network. Since there are huge amount of disconnected parts in a certain state transition graph, the entire characteristic length l has a relatively small range as shown in Fig. 7. However, it is noteworthy that few dots (or states) are connected by the state transfer lines when the power grid has a low utilization ratio (e.g., 0.1), suggesting that the power grid is stable and robust to external disturbances. The characteristic length increases when the power grid operates at higher load levels (or larger utilization ratios), and the state transition graph shows higher degrees of connectivity. This suggests the power grid is prone to cascading failures at higher load levels, which parallels to what one might deduce from institutive reasoning. It can be seen from Fig. 7 that the value of characteristic length declines after the load level exceeds a certain critical point. This is the case when the real power system operates near the critical point, most part of the power system crashes directly except for these involved in the cascading failure. From the system point of view, parameters other than the load level (e.g., number of initially failed equipments) may also cause phase transition. In essence, external disturbances, whether they are man-made or natural, change the states of network. Although it is still not clear whether and how a disturbance can cause cascading failure, the characteristic length of state transition graph could help us better understand the nature of cascading failures.

5. Conclusions

This paper analyzed the stability performance and system reliability of power grids under cascading failures. Characteristic lengths of the state transition graphs are employed to measure the stability performance of power grids at various load levels. The system reliability or availability of distribution nodes is identified as disjoint cut sets or link sets by use of the advanced network analysis algorithms such as RDA and the MSR method. The probability of each disjoint link set or cut set is computed by use of the matrix-based system reliability method. The proposed methodology is demonstrated through a case study of the HPGC power network in Hainan, China. It is found that a cascading failure could be triggered by an intentional disturbance and causes much severe consequences than a magnitude 7 earthquake. The findings could be useful for power industries and policy makers to evaluate the risk of blackout induced by cascading failures, to identify the vulnerability of power systems, and improve the resilience of power systems to external disturbances.

Inevitably, this paper has its limitations. The scope is limited to high voltage transmission network only. Nevertheless, this methodology can be extended to include distribution networks with the multi-scale analysis approach and refined network representation. In addition, the reliability of overloaded equipments and uncertainties of external disturbances are not covered in this paper. Most of distribution generation (DG) sources are installed at distribution network level. Therefore, DG has a more significant impact on system reliability at distribution network level than at the transmission network level (as the case discussed in this paper) [49], while faults at distribution network level should be isolated successfully by modern power system protection and control. Nevertheless, the distributed energy will definitely affect the power systems at transmission network level, and high penetration of DG further introduces randomness into power system analysis. For this reason, modern power system reliability analysis has to deal with such DG factors. One of the most remarkable effects of DG is the interaction between transmission network and the "active" distribution networks. In other words, the distribution network with installed DG will no longer behave as a mere power absorber, and the output of DG will affect the behavior of transmission network from a macroscopic point of view [50]. Theory of reliability analysis of such transmission network with high penetration of DG is far from perfect, and is out of the scope of this paper. Further research is in progress to incorporate the internal uncertainties (i.e., reliability electrical equipments) and uncertainties in external disturbances.

Acknowledgments

Both authors are awarded the CSSS scholarships to attend the Santa Fe Institute Complex Systems Summer School (CSSS'06). The authors gratefully acknowledge the financial support from the Santa Fe Institute, and the National Natural Science Foundation of China under Grant No. 50337010 (Z. Wu).

References

[1] Alguacil N, Carrión M, Arroyo JM. Transmission network expansion planning under deliberate outages. Int J Electr Power Energy Syst 2009;31:553–61.
[2] US–Canada Power System Outage Task Force. Final report on the August 14, 2003 blackout in the United States and Canada: Causes and recommendations; 2004. <https://reports.energy.gov/BlackoutFinal-Web.pdf>.
[3] Chang SE, Seligson HA, Eguchi RT. Estimation of the economic impact of multiples lifeline distribution: Memphis light, gas and water division case study. Technical report NCEER-96-001. Buffalo (NY): National Center for Earthquake Engineering Research (NCEER); 1996.
[4] Chang SE, Rose AZ, Shinozuka M, Tierney KJ. Modeling earthquake impact on urban lifeline systems: advances and integration in loss estimation. In: Earthquake engineering frontiers in the new millennium. Netherlands: Swets & Zeitlinger; 2001.
[5] Wu Z, Chang L, Shi S. Reliability analysis of power systems under disaster impacts. Santa Fe Institute complex systems summer school (CSSS 06) final report; 2006. <http://tuvalu.santafe.edu/events/workshops/images/e/e2/Bj_csss06_zhigang_et_al.pdf>.
[6] Zhou X, Yan C. A blackout in Hainan Island power system: causes and restoration procedure. In: Proceedings of 2008 IEEE power and energy society general meeting, Pittsburgh, Pennsylvania, July 20–24, 2008.
[7] Nuti C, Rasulo A, Vanzi I. Seismic safety evaluation of electric power supply at urban level. Earthq Eng Struct Dyn 2007;36(2):245–63.
[8] Shinozuka M, Dong X, Cheng TC, Jin X. Seismic performance of electric transmission network under component failures. Earthq Eng Struct Dyn 2007;36(2):227–44.
[9] LaCommare KH, Eto JH. Understanding the cost of power interruptions to U.S. electricity customers (LBNL-55718). Berkeley (CA): Lawrence Berkeley National Laboratory; 2004.
[10] Maharana MK, Swarup KS. Graph theoretic approach for preventive control of power systems. Int J Electr Power Energy Syst 2010;32:254–61.
[11] Helseth A, Holen AT. Structural vulnerability of energy distribution systems: incorporating infrastructural dependencies. Int J Electr Power Energy Syst 2009;31:531–7.
[12] Carreras BA, Lynch VE, Dobson I, Newman DE. Critical points and transitions in an electric power transmission model for cascading failure blackouts. Chaos 2002;12(4):985–94.
[13] Dobson I, Chen J, Thorp JS, Carreras BA, Newman DE. Examining criticality of blackouts in power system models with cascading events. In: Proceedings of 35th annual Hawaii international conference on system sciences (HICSS), Hawaii, January 7–10, 2002.
[14] Nedic DP, Dobson L, Kirschen DS, Carreras BA, Lynch VE. Criticality in a cascading failure blackout model. Int J Electr Power Energy Syst 2006;28:627–33.
[15] Wu Z, Zhong Q, Zhang Y. State transition graph of cascading electrical power grids. In: Proceedings of IEEE power engineering society general meeting, Tampa, Florida, USA, June 24–28, 2007.
[16] Watts DJ. Small worlds: the dynamics of networks between order and randomness. Princeton (NJ): Princeton University Press; 1999.
[17] Rosas-Casals M, Solé R. Analysis of major failures in Europe's power grid. Int J Electr Power Energy Syst 2011;33(21):805–8.
[18] Barabasi AL. Linked: the new science of networks. Cambridge (MA): Perseus Publishing; 2002.
[19] Li J. Lifeline earthquake engineering: theories and applications. Beijing (China): Science Press; 2005.
[20] Vanzi I. Seismic reliability of electric power networks: methodology and application. Struct Safety 1996;18(4):311–27.
[21] Kroft D. All paths throughout a maze. Proc IEEE 1967;55:88–90.
[22] Panoussis G. Seismic reliability of lifeline networks (MIT-CE R74-57). SDDA report no. 15. Cambridge (MA): Department of Civil Engineering, Massachusetts Institute of Technology; 1974.
[23] Taleb-Agha G. Seismic risk analysis of lifeline networks (MIT-CE R75-49). Cambridge (MA): Department of Civil Engineering, Massachusetts Institute of Technology; 1975.
[24] Taleb-Agha G. Seismic risk analysis of lifeline networks. Bull Seism Soc Am 1977;67:1625–45.
[25] Aggarwal KK, Misra KB. A fast algorithm for reliability evaluation. IEEE Trans Reliab 1975;24(1):83–5.
[26] Dotson WP, Gobien JO. A new analysis technique for probability graphs. IEEE Trans Circ Syst 1979;26:855–65.
[27] Yoo YB, Deo N. A comparison of algorithm for terminal-pair reliability. IEEE Trans Reliab 1988;37:210–5.
[28] Torrieri D. Calculation of node-pair reliability in large networks with unreliable nodes. IEEE Trans Reliab 1994;43:375–7.
[29] Li J, He J. A recursive decomposition algorithm for network seismic reliability evaluation. Earthq Eng Struct Dyn 2002;31:1525–39.
[30] Wu X, Sha J. Full probability decomposition algorithm for network reliability. Syst Eng Electron Technol (China) 1998;6:71–3.
[31] Kuo S, Lu S, Yeh F. Determining terminal-pair reliability based on edge expansion diagram using OBDD. IEEE Trans Reliab 1999;R48:234–46.
[32] Ditlevsen HA. Narrow reliability bounds for structural systems. J Struct Mech ASCE 1979;7(4):453–72.
[33] Song J, Der Kiureghian A. Bounds on system reliability by linear programming. J Eng Mech ASCE 2003;129(6):627–36.
[34] Song J, Der Kiureghian A, Sackman JL. Seismic response and reliability of electrical substation equipment and systems. Berkeley (CA): Pacific Earthquake Engineering Research (PEER) Center, University of California; 2004.
[35] Chang L, Song J. Matrix-based reliability analysis of urban infrastructure networks: a case study of MLGW natural gas network. In: Proceedings of the 5th China–Japan–US trilateral symposium on lifeline earthquake engineering, Haikou, China, November 26–28, 2007.
[36] Song J, Kang W-H. Matrix-based system reliability method and applications to structural systems. In: Proceedings of the 18th ASCE engineering mechanics division conference, Blacksburg, Virginia, USA, June 3–6, 2007.
[37] Taylor CW. Power system voltage stability. New York: McGraw-Hill Education; 1994.
[38] Wuensche A. Basins of attraction in network dynamics: a conceptual framework for biomolecular networks. In: Modularity in development and evolution. Chicago (IL): Chicago University Press; 2003.
[39] Kang W-H, Song J, Gardoni P. Matrix-based system reliability method and applications to bridge networks. In: Proceedings of the 10th international conference on applications of statistics and probability in civil engineering (ICASP), Tokyo, Japan, July 31–August 3, 2007.
[40] Song J, Der Kiureghian A. Component importance measures by linear programming bounds on system reliability. In: Proceeding of the 9th international conference on structural safety and reliability (ICOSSAR), Rome, Italy, June 19–23, 2005.
[41] Der Kiureghian A, Song J. Multi-scale reliability analysis and updating complex systems by use of linear programming. Reliab Eng Syst Safety 2008;93(2):288–97.
[42] Araneda JC, Rudnick H, Mocarquer S, Miquel P. Lessons from the 2010 Chilean earthquake and its impact on electricity supply. In: 2010 international conference on power system technology (PowerCon 2010), Hangzhou, China, October 24–28, 2010.
[43] National Population and Family Planning Commission of China (NPFPCC). Data available from NPFPCC; 2006. <http://www.chinapop.gov.cn/cms/export/sites/chinapop/rkxx/gdkx/t20060410_58183.htm>.
[44] Hainan Power Grid Company (HPGC). Brief introduction of HPGC facts. Report available at HPGC website; 2007. <http://www.hn.csg.cn/gaikuang/>.
[45] Der Kiureghian A. Bayesian method for seismic fragility assessment of lifeline components. In: Acceptable risk process – lifelines and natural hazards. Reston (VA): ASCE; 2002.
[46] Gilani AS, Whittaker AS, Fenves GL, Chen C-H, Ho H. Seismic evaluation and analysis of 230 kV disconnect switches. PEER report 2000/06. Berkeley (CA): University of California; 2000.
[47] Foschi RO. Reliability theory and applications to risk analysis of power components and systems. Int J Electr Power Energy Syst 2004;26:249–56.
[48] Liu C, Lin G, Li H, Zhou J. Introduction to lifeline earthquake engineering. Dalian (China): Dalian University of Technology Press; 2005.
[49] Chowdhury AA, Agarwal SK, Koval DO. Reliability modeling of distributed generation in conventional distribution systems planning and analysis. IEEE Trans Ind Appl 2003;39(5):1493–8.
[50] Papaefthymiou G, Houwing M, Weijnen MPC, van der Sluis L. Distributed generation vs bulk power transmission. In: Proceedings of first international conference on infrastructure systems and services, November 10–12. Netherlands: Rotterdam; 2008.